Texas A&M University

Department of

METEOROLOGY

Research Conducted through the
Texas A&M Research Foundation
College Station, Texas
Project 3214

STUDY ON STEADY STATE WIND AND TURBULENCE ENVIRONMENTS

FINAL REPORT

Contract No. NAS 8-31234
Prepared by
Kenneth C. Brundidge
February, 1977

Research sponsored by
the George C. Marshall
Space Flight Center,
Alabama

STUDY ON STEADY STATE WIND AND TURBULENCE FNVIRONMENTS

CONTRACT NO. NAS 8-31234

FINAL REPORT

February, 1977

Prepared by

Kenneth C. Brundidge

Department of Meteorology

Texas A&M University

for

Texas A&M Research Foundation

P.O. Faculty Exchange H

College Station, Texas 77843

This report was prepared by Texas A&M University under Contract NAS 8-31234, "Study on Steady State Wind and Turbulence Environments," for the George C. Marshall Space Flight Center, Alabama 35812.

TABLE OF CONTENTS

INTRODUCTION

Nature of the Problem

It is well-known that aircraft can be greatly affected by cross-winds and gusts during take-off or landing.

The situation is particularly critical for vertical and/or short take-off and landing (V/STOL) aircraft which may be operating in congested urban locations and thus subjected to the wakes of hangars or tall buildings.

Wakes are regions in which the mean velocity is less but the turbulence is greater than that in the unaffected flow. Semi steady state vortices may be a feature of the wake in the near vicinity of the structure.

Aside from these general statements, little is known about the wakes of real structures in natural atmospheric flow. It follows that potentially hazardous situations for aircraft operations conceivably could be avoided if there was greater knowledge of the structure of wakes and how that structure is related to obstacle size and shape, and ambient wind.

Past Studies

Frost (1973) has provided a very useful review of over 50 papers and symposia proceedings dealing with air flow over bluff obstacles. His review reveals that studies of models in low-turbulence wind tunnels constitute by far the greater portion of the literature on the subject. These studies deal with flow over plates, forward or rear facing steps, or buildings.

Typical of the sort of flow found over buildings or plates is that given by Halitsky (1968) and shown here as Figure 1.

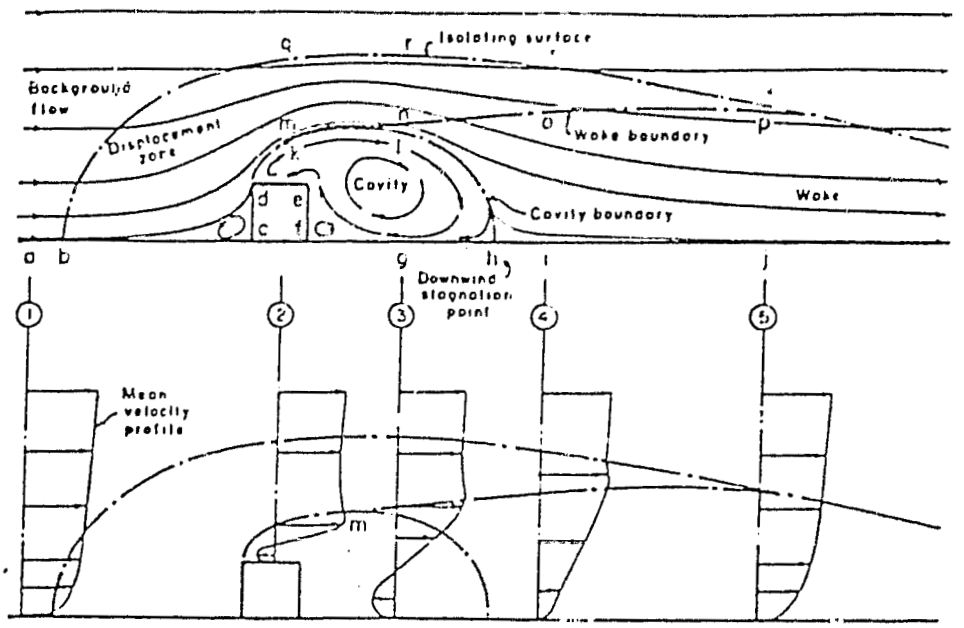

Figure 1. - Flow zones near a sharp-edged building (Halitsky, 1968).

It is seen that flow separation occurs near the forward edge of the building roof and that reattachment occurs at some distance downstream within the wake. A closed circulation is thus delineated which has been variously called, a cavity, a bubble, or an eddy.

Evans (1957) has concentrated on determining the dimensions of this feature of the wake in a wind tunnel study of buildings of various shapes and roof types. In addition, he shows that the flow pattern in the horizontal plane not only depends upon the shape of the structure but varies considerably with the orientation with respect to the wind. Unfortunately, he made no attempt to develop

analytical relationships in this study.

Halitsky provides equations dealing with the wake dimensions and mean longitudinal velocity distribution, but they are applicable to a suspended plate and therefore of limited value for the natural setting. A very elegant theoretical treatment for the flow in the vertical plane is given by Counihan et al. (1974).

The numerical simulation studies of flow around buildings (Hirt and Cook, 1972; Hotchkiss, 1972; Thomas, 1971; Frost, et al., 1973) show results similar to those of the wind tunnel studies.

It is generally agreed that wakes in the natural setting may differ considerably from those obtained in the wind tunnel or by numerical simulation. This is because the real wind in passing over the surface boundary is itself extremely turbulent and subject to random variations in speed and direction. Unfortunately, little work has been done in the natural setting. Sexton (1971) describes measurements made on the upwind side of a building which show a downwash vortex (see Figure 1) extending about one building height upstream. Measurements of average wind speed at the 3-m level above ground show reasonable agreement with wind tunnel data.

A measurement program in the wake of an airport hangar has been reported by Colmer (1971). Instrumented masts were placed along a line perpendicular to and through the middle of the long side of the hangar at distances of 5, 14, and 23 building heights (10 m). Another instrumented tower 190 m upstream provided reference data. Measurements made during a single 40-min run give indications of the extent of the wake, the intensity of the turbulence, and gradients of the

mean flow within the wake.

Purposes of Study

The present study was intended as a feasibility experiment to determine the extent to which a research aircraft could be used as a rapid-turnaround, data-acquisition system to yield useful data for aeronautical safety applications. Such a system could be used to probe the wake from many buildings and obstacles and would avoid the laborious and time-consuming method of measurements obtained from towers.

It is evident that the starting point in such an experiment would be the establishment of standard data against which to compare the aircraft data. This can be done only by making measurements in a wake with instrumented towers and developing a model based upon the pertinent parameters of the flow. The next problem would be the determination of some readily-obtainable parameters in the response of the aircraft which indicate the likely structure of the wake.

Approach to Study

One obvious signature of wake flow would be the greatly enhanced turbulence at its boundaries and interior. Studies have been published of the response of an aircraft to a field of turbulence, e.g., Jones (1969) and Kaynes (1971). However, for this to be a fruitful approach, it is required that the turbulence be homogeneous and steady state.

Furthermore, as Colmer (op. cit.) points out, a conventional aircraft at take-off or landing speed would pass through the wake of an isolated structure in one to two sec. The response of the aircraft

would not be to the energy of the turbulence at various frequencies, but rather to the gradient of mean wind speed across the wake. A VTOL aircraft could be affected by the turbulence but the gradient of mean windspeed in the wake again is expected to be the dominant factor.

Therefore, the main thrust of this study has been to obtain mean values of the flow. The intention was to use these measurements in conjunction with theoretical relationships developed by means of dimensional analysis to establish a model of the flow in the wake.

The flight program was never accomplished. This was due in part because of down-time of the aircraft, in part because of delays in getting the aircraft instrumented, but mainly because the appropriate meteorological conditions (east winds) did not occur at times when the aircraft was operational and available.

EXPERIMENT DETAILS

Study Site

The experimental site was a large hangar (100 ft x 123 ft x 40 ft) at what had been a U.S.A.F. airbase at Bryan, Texas, but which now is a property of Texas A&M University.

Figure 2 shows the site. The area to west of the hangar is a concrete apron to a distance of about 600 ft. The area surrounding the hangar on the north, east and south sides is grassy field. Some one-story buildings lie 330 ft to the north of the hangar and two more are shown to the south-southeast. Also shown on the north side of the building are a small shed, a trailer truck and what had been the flight control tower, a steel girder structure about 70 ft high.

The climatology of the area is such that the prevailing wind is southerly from late spring through early fall. However, the most open and suitable area for setting up instruments and carrying out flight measurements is the apron. Therefore, an array of spots in a polar co-ordinate grid were painted on the concrete. These were numbered and lettered as shown in Figure 2. Favorable wind directions for experimentation would be those from northeast through southeast, conditions which prevail infrequently, but occasionally after a cold-front passage.

A second grid was laid out on the south side of the building, as shown in Figure 2, to permit measurements during northerly flow. This condition is more common after cold-front passages in the area. Flight measurements in this area were ruled out because of power lines which would intersect any desirable flight path.

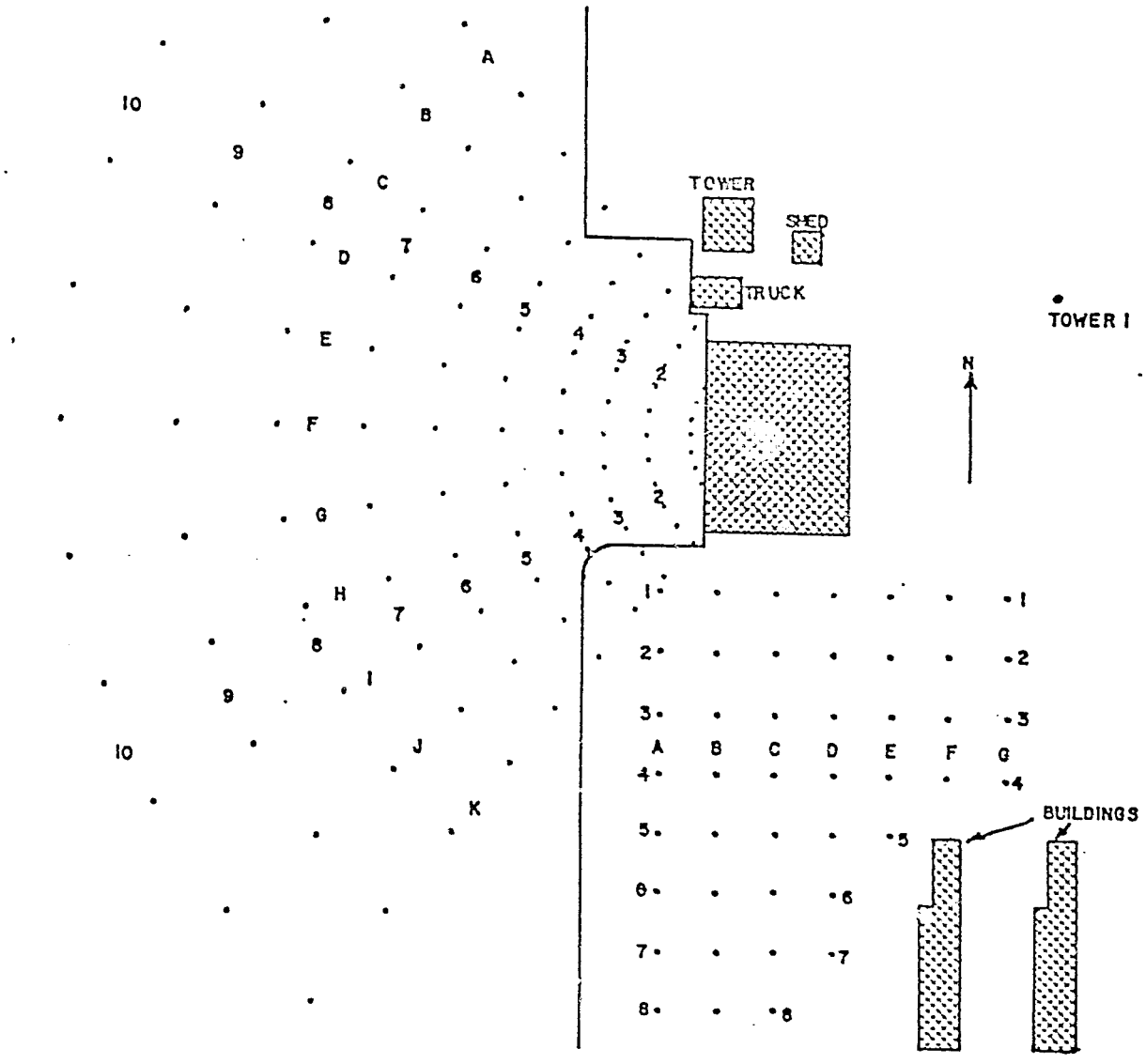

Figure 2 - Experimental site. Points represent grids used to locate instruments. Points are 40 ft apart in south grid.

Ground Measurements

The instrumentation employed was the Climet system for measurement of wind speed (model 011-1) and direction (model 012-1). Gill propeller anemometers (model 27100) were used to measure vertical motion. The instruments were mounted either on portable tripods for measurements up to 10 ft above the ground or on three large towers each with a heavy base mounted on wheels. These towers could be moved with a small tractor over even ground; furthermore, winches on these towers permitted instrument placement at any height from about 5 ft to 60 ft above ground. The unevenness and softness of the ground made it impossible to use these towers south of the hangar.

An earlier project was carried out in 1973-74. During that phase of the work one of the towers was permanently located at a point 150 ft to the east-northeast of the hangar (see Tower 1 in Figure 2). During 1975-76 the towers were unavailable most of the time. Consequently, a tripod generally was used for the upwind measurement and the placement varied from one experiment to another.

All experiments were composed of a series of approximately 15-min runs with data measured simultaneously at four or five locations. One set of instruments was always upstream from the building; these measurements were considered to be the reference or free-stream values. The intention was to operate within or at the edges of the wake with the other towers or tripods. After each run the towers and/or tripods could be relocated and on the tall towers the instruments could be moved to a new height. Thus, with fairly steady wind for two-three hours, the wake could be probed in a number of places.

The recording system, analog tape units, was located in the northeast corner the hangar. Thus, 500-ft cable lengths permitted instrument placement out to about 400 ft to the west or south of the building.

A number of problems were encountered with the recording of data on tapes and the later conversion of the data from analog to digital form. Consequently, many data were lost, e.g., all vertical motion data for the experiments run in 1975-76. It was finally decided in the spring of 1976 to abandon the use of the tape recorder and a switch was made to chart recorders.

RESULTS OF THE STUDY

Experimental Data

Those data that were recorded on magnetic tape were processed as follows. Analog values were taken from the tapes at each tenth of a second and averaged to give a 1-sec value. The 1-sec values were transformed to digital form and stored on a second tape for further analyses by computer.

The results from three experiments done in 1974 are presented in Table 1. The columns in the table show the following, going from left to right: (1) the date of the experiment and the run number, (2) the tower numbers, (3) the location of the given tower within the grid (see Figure 2), (4) the height above ground of the instruments on the given tower, (5)-(6) the average wind speed and direction in the meteorological system, and (7) the average vertical motion. The vertical motion for Tower 2 is missing for all three experiments. A W or an S has been used as a prefix in column 3 of Table 1 to indicate whether the observation site was in the "west grid" or the "south grid."

The data obtained during 1975-1976 are shown in Table 2. The experiment on 6-6-76 was the only one for which the west grid was used. For the experiments on 11-12-75 and 6-6-76, the recording of data was accomplished by Esterline-Angus chart recorders, as explained previously.

Table 1. - 1974 Experiments

Date and Run	Tower	Location	Instr. Ht. (ft)	Wind Speed (m/sec)	Wind Dir (deg)	Vertical Motion (cm/sec)
4-17-74 8	1	Fixed	8	3.0	11.5	3.7
	2	S-A3	8	2.4	16.0	---
	3	S-B3	8	2.2	6.2	-0.1
	4	S-C3	8	2.2	30.2	0.8
	5	S-D3	8	3.1	22.2	-2.0
4-23-74 1	1	Fixed	8	2.5	29.9	-3.2
	2	W-J4	8	1.8	47.0	---
	3	S-A2	8	1.3	355.0	-10.4
	4	S-B2	8	1.0	11.5	-4.6
	5	S-C2	8	1.7	58.0	18.3
4-24-74 1	1	Fixed	8	2.0	75.9	-0.6
	2	W-F5	30	1.8	88.8	---
	3	W-F5	60	3.2	188.6	-2.8
	4	W-E5	8	1.7	86.4	-9.4
	5	W-G5	8	1.5	94.6	-1.1

Table 2. - 1975-76 Experiments

Date and Run	Tower	Location	Instr. Ht. (ft)	Wind Speed (m/sec)	Wind Dir (deg)
10-16-75					
1	1	Fixed	8	6.8	333.4
	2	B1	8	3.1	351.8
	4	C1	8	3.1	101.7
2	1	Fixed	8	5.1	337.3
	2	C2	8	1.3	68.0
	4	D2	8	2.8	49.5
3	1	Fixed	8	3.6	343.7
	2	E3.5	8	3.2	4.6
	4	F3.5	8	4.1	351.7
	5	G3.5	8	4.4	342.5
10-17-75					
1	1	Fixed	8	3.4	335.0
	2	B1	8	1.0	346.4
	4	C1	8	1.1	91.7
	5	D1	8	2.8	82.2
2	1	Fixed	8	5.2	334.3
	2	E2	8	2.2	12.8
	4	F2	8	3.8	331.5

Table 2. - Continued

Date and Run	Tower	Location	Instr. Ht. (ft)	Wind Speed (m/sec)	Wind Dir (deg)
3	1	Fixed	8	5.4	317.5
	2	E3	8	2.2	16.6
	4	F3	8	4.7	340.5
4	1	Fixed	8	6.0	310.0
	2	E4	8	2.5	9.5
	4	F4	8	5.0	340.9
5	1	Fixed	8	6.0	321.9
	2	D4	8	3.1	19.7
	4	E3	8	4.6	350.0
6	1	Fixed	8	5.3	301.3
	2	E1	8	2.2	27.1
	4	F2	8	4.1	336.1
11-12-75					
2	1	Fixed	8	8.7	324.6
	2	C3	8	4.1	27.0
3	1	Fixed	8	8.7	319.1
	2	B6	8	7.1	346.4

Table 2. - Continued

Date and Run	Tower	Location	Instr. Ht. (ft)	Wind Speed (m/sec)	Wind Dir (deg)
6-6-76					
1	1	Fixed	8	2.9	49.7
	2	W-K7	8	2.8	45.8
2	1	Fixed	15	3.2	51.5
	2	W-K7	8	2.7	61.4
3	1	Fixed	30	3.7	56.1
	2	W-K7	30	4.2	70.4
4	1	Fixed	60	3.2	48.6
	2	W-K7	60	3.6	58.9
5	1	Fixed	8	2.4	65.6
	2	W-G9	8	2.8	63.8
6	1	Fixed	15	2.9	63.6
	2	W-G9	15	3.0	71.1
7	1	Fixed	30	3.7	54.9
	2	W-G9	30	4.1	60.2

Table 2. - Continued

Date and Run	Tower	Location	Instr. Ht. (ft)	Wind Speed (m/sec)	Wind Dir (deg)
8	1	Fixed	8	3.5	60.9
	2	W-H6	8	2.7	69.6
9	1	Fixed	15	3.6	72.5
	2	W-H6	15	2.6	73.3
10	1	Fixed	30	3.2	57.3
	2	W-H6	30	3.0	54.9
11	1	Fixed	60	3.8	63.7
	2	W-H6	60	3.9	65.9

Theoretical Development.

We first establish the nature of the equations which must be used in the analysis by a scaling procedure, along the lines of that given by Tennekes and Lumley in their discussion of the turbulent wake (A First Course in Turbulence, pp. 104-109).

Accordingly, we start with the equations of mean motion and the continuity equation (the coriolis terms and molecular viscosity terms are neglected):

$$\frac{\partial U}{\partial t} + U\frac{\partial U}{\partial x} + V\frac{\partial U}{\partial y} + W\frac{\partial U}{\partial z} = -\frac{1}{\rho}\frac{\partial P}{\partial x} - \frac{1}{\rho}\left[\frac{\partial}{\partial x}\overline{\rho u^2} + \frac{\partial}{\partial y}(\overline{\rho uv}) + \frac{\partial}{\partial z}(\overline{\rho uw})\right], \quad (1)$$

$$\frac{\partial V}{\partial t} + U\frac{\partial V}{\partial x} + V\frac{\partial V}{\partial y} + W\frac{\partial V}{\partial z} = -\frac{1}{\rho}\frac{\partial P}{\partial y} - \frac{1}{\rho}\left[\frac{\partial}{\partial x}(\overline{\rho uv}) + \frac{\partial}{\partial y}(\overline{\rho v^2}) + \frac{\partial}{\partial z}(\overline{\rho vw})\right], \quad (2)$$

$$\frac{\partial W}{\partial t} + U\frac{\partial W}{\partial x} + V\frac{\partial W}{\partial y} + W\frac{\partial W}{\partial z} = -\frac{1}{\rho}\frac{\partial P}{\partial z} - g - \frac{1}{\rho}\left[\frac{\partial}{\partial x}(\overline{\rho uw}) + \frac{\partial}{\partial y}(\overline{\rho vw}) + \frac{\partial}{\partial z}(\overline{\rho w^2})\right], \quad (3)$$

$$\frac{\partial U}{\partial x} + \frac{\partial V}{\partial y} + \frac{\partial W}{\partial z} = 0 \quad (4)$$

At this point, we assume that the flow in the wake is similar to that shown in Figures 3 and 4. In these drawings, two scale lengths are introduced. The first, ℓ_1, corresponds to that defined by Tennekes and Lumley as the point at which $U-U_0 \simeq \frac{1}{2} U_s$. The scale length, ℓ_2, in the z direction follows from the discussion of Chang's wind tunnel work by Plate (pp. 162-165). It marks the surface of $U=\frac{1}{2} U_0'$. It follows that both ℓ and ℓ_2 are functions of x.

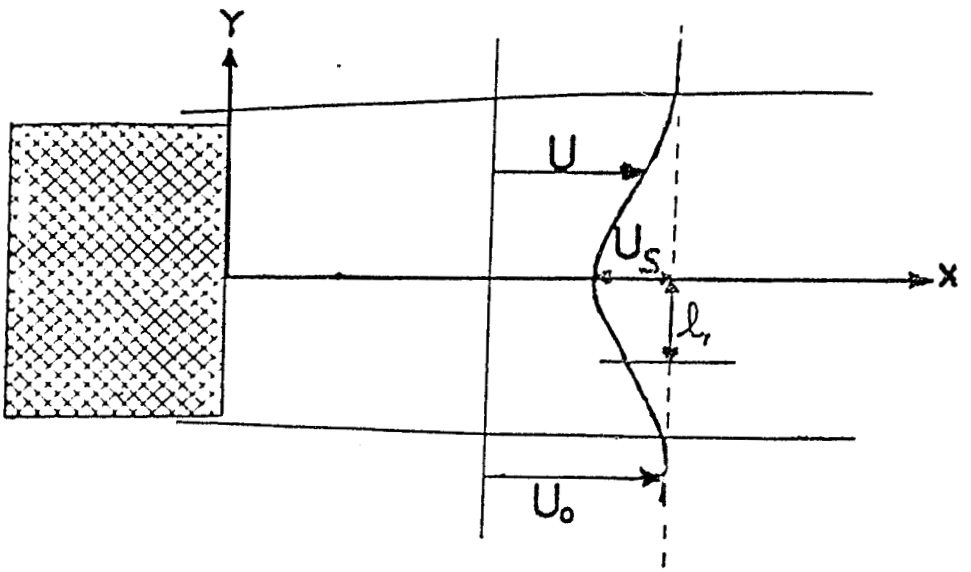

Figure 3. - Hypothesized characteristics of wake flow in x, y plane.

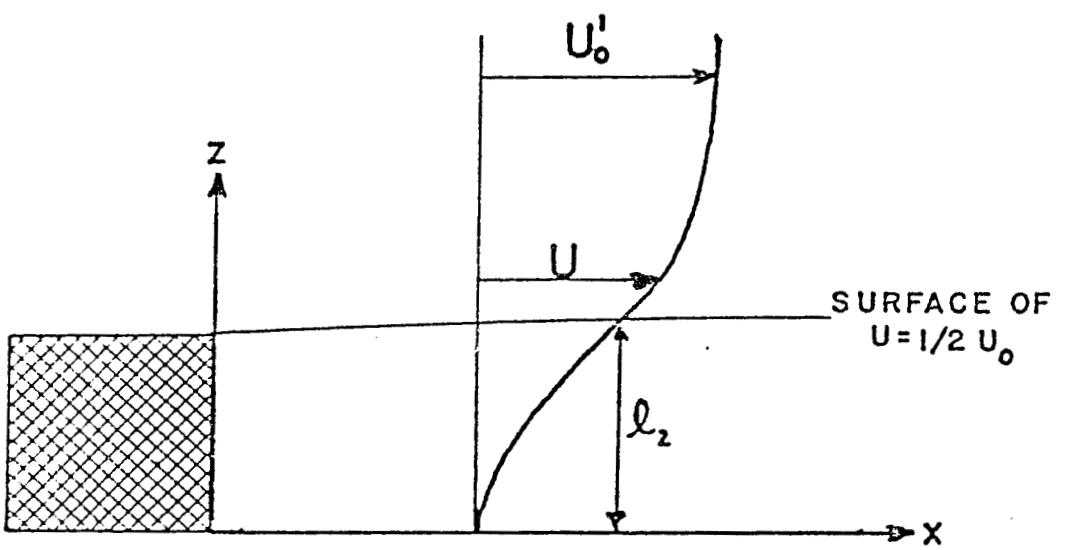

Figure 4. - Hypothesized characteristics of wake flow in x, z plane.

Then, following Tennekes and Lumley, we can say that

$$\frac{\partial U}{\partial y} = \mathcal{O}(U_s/\ell_1) \text{ and } \frac{\partial U}{\partial x} = \mathcal{O}(U_s/L) \ , \tag{5}$$

where L denotes a scale length in the X direction. From the continuity equation, the orders of magnitude are:

$$\frac{U_s}{L} + \frac{V}{\ell_1} + \frac{W}{\ell_2} = 0$$

Assume: $\frac{V}{\ell_1} \sim \frac{U_s}{L}$ and $\frac{W}{\ell_2} \sim \frac{1}{10}\frac{U_s}{L}$,

where $\mathcal{O}(\ )$ and $\sim$ signify order of magnitude.

Therefore,

$$V = \mathcal{O}\left(\frac{U_s \ell_1}{L}\right) \ , \ W = \mathcal{O}\left(\frac{U_s \ell_2}{10L}\right) \ . \tag{6}$$

We now assume that $U_s \sim \frac{1}{10} U_0$, $\ell_1 \sim \frac{1}{10} L$, and $U_0 \sim U_0$. Then, assuming steady state conditions and comparing the magnitudes of the terms in (1) gives:

$$\frac{U\partial U}{\partial x} \sim U_0\left(\frac{U_s}{L}\right) \sim \frac{1}{10} \ \frac{U_0^2}{10\ell_1} = \frac{U_0^2}{100\ell_1} \ ,$$

$$V \frac{\partial U}{\partial y} \sim \frac{U_s \ell_1}{L}\left(\frac{U_s}{\ell_1}\right) = \frac{U_s^2}{L} \sim \frac{U_0^2}{1000\ell_1} \ ,$$

$$W \frac{\partial U}{\partial z} \sim \left(\frac{U_s \ell_2}{10L}\right)\frac{U_0}{\ell_2} = \frac{U_0 U_s}{10L} \sim \frac{1}{10}\frac{U_0^2}{100\ell_1} \ ,$$

$$\frac{\overline{\partial u^2}}{\partial x} \sim \frac{u^2}{L} \sim \frac{U_0^2}{1000\ell_1} \ ; \text{ where it was assumed } u \sim \frac{1}{10} U_0 \ ,$$

$$\left.\begin{aligned} \frac{\partial \overline{uv}}{\partial y} &\sim \frac{u^2}{\ell_1} \sim \frac{1}{100}\frac{U_0^2}{\ell_1}, \\ \frac{\partial \overline{uw}}{\partial z} &\sim \frac{u^2}{\ell_2} \sim \frac{1}{100}\frac{U_0^2}{\ell_2} \end{aligned}\right\} \quad \text{since } v, w \sim u$$

Therefore, the approximation to (1) is

$$U\frac{\partial U}{\partial x} + \frac{\partial \overline{uv}}{\partial y} + \frac{\partial \overline{uw}}{\partial z} = -\frac{1}{\rho}\frac{\partial P}{\partial x} \quad . \tag{7}$$

Equation (2) terms become:

$$U\frac{\partial V}{\partial x} \sim U_0\left(\frac{U_s \ell_1}{L}\right)\frac{1}{L} = \frac{U_0 U_s \ell_1}{L^2} = \frac{U_0^2}{1000\ell_1} \quad ,$$

$$V\frac{\partial V}{\partial y} \sim \left(\frac{U_s \ell_1}{L}\right)\frac{1}{\ell_1} = \frac{U_s^2 \ell_1}{L^2} = \frac{U_0^2}{1000\ell_1} \quad ,$$

$$W\frac{\partial V}{\partial z} \sim \left(\frac{U_s \ell_2}{10L}\right)\left(\frac{U_s \ell_1}{L}\right)\frac{1}{\ell_2} = \frac{U_s^2 \ell_1}{10L^2}\ \frac{1}{10000}\ \frac{U_0^2}{\ell_1} \quad ,$$

$$\frac{\partial \overline{uv}}{\partial x} \sim \frac{u^2}{L} \sim \frac{1}{100}\ \frac{U_0^2}{L} \sim \frac{U_0^2}{1000\ell_1} \quad ,$$

$$\frac{\partial \overline{v^2}}{\partial y} \sim \frac{u^2}{\ell_1} \sim \frac{U_0^2}{100\ell_1} \quad ,$$

$$\frac{\partial \overline{vw}}{\partial z} \sim \frac{u^2}{\ell_2} \sim \frac{U_0^2}{100\ell_2} \sim \frac{U_0^2}{100\ell_1} \qquad (\text{Note, } \ell_1 \sim \ell_2).$$

Then, (2) becomes: $\dfrac{\partial \overline{v^2}}{\partial y} + \dfrac{\partial \overline{vw}}{\partial z} = -\dfrac{1}{\rho}\dfrac{\partial P}{\partial y}$. (8)

From (3),

$$U\frac{\partial W}{\partial x} \sim U_o\left(\frac{U_s \ell_2}{10L}\right)\frac{1}{L} = \frac{U_0 U_s \ell_2}{10L^2} \sim \frac{U_0^2}{10{,}000\ell_2}$$

$$V \frac{\partial W}{\partial y} \sim \frac{U_s \ell_1}{L} \quad \frac{1}{10} \left(\frac{U_s \ell_2}{L}\right) \frac{1}{\ell_1} = \frac{U_s^2 \ell_2}{L^2} \sim \frac{U_0^2}{10{,}000 \ell_2} ,$$

$$W \frac{\partial W}{\partial z} \sim \left(\frac{U_s \ell_2}{10L}\right)^2 \frac{1}{\ell_2} = \frac{U_s^2 \ell_2}{100L^2} \sim \frac{U_0^2}{10^6 \ell_2} ,$$

$$\frac{\partial \overline{uw}}{\partial x} \sim \frac{u^2}{L} \sim \frac{1}{10\ell_1} \left(\frac{U_0^2}{100}\right) \sim \frac{U_0^2}{1000\ell_1} ,$$

$$\frac{\partial \overline{vw}}{\partial y} \sim \frac{u^2}{\ell_1} \sim \frac{U_0^2}{100\ell_1} ,$$

$$\frac{\partial \overline{w^2}}{\partial z} \sim \frac{u^2}{\ell_2} \sim \frac{U_0^2}{100\ell_2} .$$

Thus, $$\frac{\partial \overline{vw}}{\partial y} + \frac{\partial \overline{w^2}}{\partial z} = - \frac{1}{\rho} \frac{\partial P}{\partial z} - g . \qquad (9)$$

We identify P' as the pressure anomaly due to the effect of the building and P_0 as hydrostatic pressure, i.e.,

$$P = P_0 + P'.$$

If we ignore synoptic effects, then we can assume $\nabla_h P_0 \simeq 0$. Also, if we assume that the mechanical effect of the building on the flow is much larger than any buoyancy effects, we can use the hydrostatic approximation. Thus,

$$U \frac{\partial U}{\partial x} + \frac{\partial \overline{uv}}{\partial y} + \frac{\partial \overline{uw}}{\partial z} = - \frac{1}{\rho} \frac{\partial P'}{\partial x} , \qquad (10)$$

$$\frac{\partial \overline{v^2}}{\partial y} + \frac{\partial \overline{vw}}{\partial z} = - \frac{1}{\rho} \frac{\partial P'}{\partial y} , \qquad (11)$$

$$\frac{\partial \overline{vw}}{\partial y} + \frac{\partial w^2}{\partial z} = - \frac{1}{\rho} \frac{\partial P'}{\partial z} . \qquad (12)$$

From Chang's work (Plate, Fig. 4.10), it may be assumed that $P' \propto U_0^2$.

Then letting

$$P' = A\,(x,y,z)\,U_0^2$$

gives:
$$\frac{1}{\rho}\frac{\partial P'}{\partial x} = \frac{\partial A}{\partial x}\,\frac{U_0^2}{\rho} = \mathcal{O}\left(\frac{A}{L'}\,\frac{U_0^2}{\rho}\right) ,$$

$$\frac{1}{\rho}\frac{\partial P'}{\partial y} = \frac{\partial A}{\partial y}\,\frac{U_0^2}{\rho} = \mathcal{O}\left(\frac{A}{\ell_1}\,\frac{U_0^2}{\rho}\right) ,$$

$$\frac{1}{\rho}\frac{\partial P'}{\partial z} = \frac{\partial A}{\partial z}\,\frac{U_0^2}{\rho} = \mathcal{O}\left(\frac{A}{\ell_2}\,\frac{U_0^2}{\rho}\right) .$$

From the previous scale analysis we must have

$$\frac{A}{L'}\,\frac{U_0^2}{\rho} \sim \frac{1}{100}\,\frac{U_0^2}{\ell_1} \text{ or } A \sim \frac{\rho}{100}\,\frac{L'}{\ell_1} ,$$

$$\frac{A}{\ell_1}\,\frac{U_0^2}{\rho} \sim \frac{1}{100}\,\frac{U_0^2}{\ell_1} \text{ or } A \sim \frac{\rho}{100} ,$$

$$\frac{A}{\ell_2}\,\frac{U_0^2}{\rho} \sim \frac{1}{100}\,\frac{U_0^2}{\ell_2} \text{ or } A \sim \frac{\rho}{100} ,$$

It is seen that if it is reasonable to expect that ℓ_1 and ℓ_2 are appropriate scale lengths for pressure as well as motion, then we must have $L'/\ell_1 = \mathcal{O}(1)$. Thus, the scale length for pressure in the X direction would have to be much smaller than that for scaling motion. On the other hand, it seems more reasonable to expect the scale length for pressure in the x direction also to be the same as that for velocity. Then, $L' \sim L \sim 10\ell_1$. Accepting the result from the second and third equations of motion that $A \sim \rho/100$ then implies that

$$\frac{1}{\rho}\frac{\partial P'}{\partial x} \sim \frac{1}{1000}\,\frac{U_0^2}{\ell_1} ,$$

which is negligible when compared to the other terms in (7).

When the Reynold's stress terms are expressed in terms of the familiar mixing length concept, the system of equations becomes:

$$U \frac{\partial U}{\partial x} - K \frac{\partial^2 U}{\partial y^2} - \frac{\partial}{\partial z}\left(K \frac{\partial U}{\partial z}\right) = 0 \quad , \tag{13}$$

$$K \frac{\partial^2 V}{\partial y^2} + \frac{\partial}{\partial z}\left(K \frac{\partial V}{\partial z}\right) = \frac{1}{\rho} \frac{\partial P'}{\partial y} \quad , \tag{14}$$

$$K \frac{\partial^2 W}{\partial y^2} + \frac{\partial}{\partial z}\left(K \frac{\partial W}{\partial z}\right) = \frac{1}{\rho} \frac{\partial P'}{\partial z} \quad , \tag{15}$$

$$\frac{\partial U}{\partial x} + \frac{\partial V}{\partial y} = 0 \tag{16}$$

At this point it is assumed that the flow in the wake is composed of a basic state plus a perturbation. The basic state is taken to be the undisturbed, upwind value U_0. Therefore,

$$U = U_0(z) + U'(x,y,z,t)$$

Furthermore, it is assumed that $U_0(z)$ can be represented by the familiar log law. Then,

$$U_0 = \frac{U*}{k} \ln \frac{z}{z_o}$$

And, $K = k\, U_* \, z$. As a consequence (13) becomes

$$U_0 \frac{\partial U'}{\partial x} - K \frac{\partial^2 U'}{\partial y^2} - \frac{\partial}{\partial z}\left(K \frac{\partial U'}{\partial z}\right) = 0 \tag{17}$$

Long (1963) and Calder (1967) have emphasized the importance of using the controlling equations when they are known for purposes of generalizing the dimensional analysis procedure. Frequently, the

number of dimensional ratios can be reduced below that obtained by the usual dimensional analysis procedure and, therefore, a more powerful relationship is obtained. Such is the case here and it is for this reason that relationships (13) - (16) were developed.

In the present instance we use the equations of motion plus the "balance equation" which is derived from the former by using the continuity equation.

Thus,

$$-\frac{1}{\rho} v^2 P' = U_0 \frac{\partial^2 U'}{\partial x^2} \tag{18}$$

We assume the following boundary conditions.

$U' = 0$ at $y = \pm Q \ell_1$

$U' = -U_0 = 0$ at $z = z_0$; $U' = 0$ at $z = H$.

$U' = 0$ at $x = \infty$; $U' = -U_0$ at $x = 0$.

$V = V_{max}$ at $y = \pm Q \ell_1$; $V = 0$ at $z = 0, H$.

$W = 0$ at $z = 0, H$; $W = 0$ at $y = \pm Q \ell_1$.

$P' = 0$ at $y = \pm Q \ell_1$ and $z = H$.

$$\frac{\partial P'/\rho}{\partial z} = \frac{\partial}{\partial z} \left(K \frac{\partial W}{\partial z} \right) \quad \text{at } z = 0 \ .$$

Here, the lateral boundary of the wake is assumed to be at $y = \pm Q \ell_1$ and H is the top of the wake. Q is a dimensionless factor. It is assumed the H is $3\ell_2$ at best and that $\ell_2 \simeq$ height of obstacle.

Following Long's procedure, let

$[X] = A$	$[U'] = D$	$[P'/\rho] = G$	$[\ell_1] = J$
$[y] = B$	$[V] = E$	$[\dot{K}] = h$	$[\ell_2] = k$
$[z] = C$	$[W] = F$	$[U_0] = I$	

When these relationships are substituted into (14) - (17), (18) and the boundary conditions, we obtain:

$$[\,X\,] = A \qquad [\,U'\,] = hAC^{-1} \qquad [\,P'/\rho\,] = h^2C^{-2}$$

$$[\,y\,] = B \qquad [\,V\,] = hB^{-1} \qquad [\,K\,] = h$$

$$[\,z\,] = r \qquad [\,W\,] = hC^{-1} \qquad [\,U_0\,] = hAC^{-2}$$

$$[\,\ell_1\,] = B \qquad [\,\ell_2\,] = C$$

It is assumed that U', V, W, and P'/ρ are all functions of x, y, z, K, U_0, ℓ_1, ℓ_2. Consequently, it is found that:

$$\frac{U'}{U_0} = f_1\left(\frac{K}{U_0 z}\cdot\frac{x}{z}, \frac{\ell_1}{y}, \frac{\ell_2}{z}\right) , \tag{19}$$

$$\frac{V}{U_0} = \frac{z^2}{xy} f_2\left(\frac{K}{U_0 z}\cdot\frac{x}{z}, \frac{\ell_1}{y}, \frac{\ell_2}{z}\right) , \tag{20}$$

$$\frac{W}{U_0} = \frac{1}{xz} f_3\left(\frac{K}{U_0 z}\cdot\frac{x}{z}, \frac{\ell_1}{y}, \frac{\ell_2}{z}\right) , \tag{21}$$

$$\frac{P'}{\rho U_0^2} = \frac{1}{x^2} f_4\left(\frac{K}{U_0 z}\cdot\frac{x}{z}, \frac{\ell_1}{y}, \frac{\ell_2}{z}\right) . \tag{22}$$

In the following we concentrate on finding the functional relationship for U' for conditions that match those under which the observations were taken. Accordingly, it is assumed that the basic flow, U_0, can be represented by the log profile, i.e.,

$$U_0 = \frac{U_*}{k} \ln z/z_0$$

for which $K = k U_* z$. Then, (17) becomes

$$\frac{U_0}{kU_*}\frac{\partial U'}{\partial x} - z\frac{\partial^2 U'}{\partial y^2} - \frac{\partial U'}{\partial z} - z\frac{\partial^2 U'}{\partial z^2} = 0. \tag{23}$$

We identify z = Z, the height of the observations so that (23) becomes,

$$\frac{U_0(Z)}{kU_*}\frac{\partial U'}{\partial x} - Z\frac{\partial^2 U'}{\partial y^2} - \frac{\partial U'}{\partial z} - Z\frac{\partial^2 U'}{\partial z^2} = 0 \quad . \tag{24}$$

Thus, the coefficients in (24) are treated as constants.

A multitude of expressions for U' were tested to see if they could serve as a solution to (24) keeping (19) in mind. One possibility is the relation

$$-U' = U_0(z)\,\bar{x}^n\,A(\xi) \quad , \tag{25}$$

where n = constant, $\bar{x} = x/h$, $\xi = y/\ell_1(\bar{x})$; h is taken to be the height of the building. When (25) is substituted into (24) we obtain

$$\frac{d^2A}{d\xi^2} + \left[\frac{U_0(Z)}{khU_*Z}\,\ell_1\,\frac{d\ell_1}{d\bar{x}}\right]\xi\,\frac{dA}{d\xi} - \left[\frac{U_0(Z)}{khU_*Z}\,\frac{\ell_1^{\,2}}{\bar{x}}\right] n\,A = 0 \quad . \tag{26}$$

We wish the solution to describe a self-preserving flow. This condition will be met if

$$\ell_1(\bar{x}) = \left(\frac{2khU_*Z}{U_0(Z)}\right)\bar{x}^{\,1/2} \quad . \tag{27}$$

Then (26) becomes

$$\frac{d^2A}{d\xi^2} + \xi\,\frac{dA}{d\xi} - 2n\,A = 0 \quad . \tag{28}$$

We expect that $A(\xi)$ should be a maximum at $\xi = 0$ and symmetric with respect to $\xi = 0$. The values of $\ell_1(\bar{x})$ for the experimental conditions in this study range from about 7 ft to 15 ft. Therefore, $A(\xi)$ should approach zero as ξ goes to plus or minus five or six. A function which will behave in this fashion is given by $B\,e^{-\alpha\xi^2}$, where B and α

are constants. When this function is substituted into (28), it is found that it will be a solution providing $\alpha = 1/2$ and $n = -1/2$. The statement for (25) then becomes,

$$-\frac{U'}{U_0(Z)}\left(\frac{x}{h}\right)^{1/2} = B\, e^{\xi^2/2} \tag{29}$$

The value of B can be determined by setting U' equal to U_s at $\xi = 0$ on a plot of the left-hand side of (29) versus ξ.

Another possible solution can be obtained by expressing $A(\xi)$ as,

$$A(\xi) = \sum_{i=0}^{\infty} a_i\, \xi^i \quad , \tag{30}$$

where the coefficients a_i are to be determined by substitution into (28). The symmetry condition requires that the final expression shall contain no odd powers of ξ. Accordingly, it is found that

$$A(\xi) = a_0 + \sum_{i=1}^{\infty} \frac{(2n-2i+2)(2n-2i+4)\cdots\cdots(2n-2)2n}{2i!}\, a_0 \xi^{2i} \tag{31}$$

where a_0 can be determined in terms of U_s by setting $\xi = 0$ when (31) is substituted into (25). The difficulty with this solution is that the value of n is not readily determined. Since $A(\xi) = 0$ at the boundary of the wake, say $\xi = \pm 6$, an infinite set of values of n would arise as roots of the equation,

$$\sum_{i=1}^{\infty} \frac{(2n-2i+2)(2n-2i+4)\cdots\cdots(2n+2)\ 2n}{(2i)!} = 0$$

It would be necessary to test each value to find the best fit for the observations - a monumental task!

A third possibility arises by a change in definition of the quantity, $\ell_1(\bar{x})$. A somewhat unsatisfying feature of the previous solutions is that the width of the obstacle is not an explicit feature of the scaling. Let $\ell_1(\bar{x})$ be redefined as L, the half-width of the cross section presented to the wind by the obstacle. L will vary as the direction of the mean reference wind varies. We assume as a solution,

$$- U' = U_0(-Q_1\xi^2 + Q_1)\, A(\bar{x}) \ . \tag{32}$$

where $\bar{x} = x/h$, $\xi = y/L$, and $h \approx \ell_2$ is the height of the structure. The quantity $(-Q_1\xi^2 + Q_1)$ represents a parabola which requires $U' = 0$ at $\xi = \pm 1$, i.e., $y = \pm L$.

When (32) is substituted into (24), it is found that

$$A(\bar{x}) = B_1 e^{-\delta_1 \bar{x}} \quad , \ B = \text{constant},$$

and

$$\delta_1 = \frac{2ZkhU_*}{L^2\, U_0(Z)(1-\xi^2)} \ .$$

It can be seen that

$$- \frac{U'\ e^{\delta_1 \bar{x}}}{U_0(Z)} = Q_1 B_1 (1-\xi^2) \ . \tag{33}$$

Finally, a solution which actually differs very little from (32) is given by

$$- U' = U_0 Q_2 \cos\left(\frac{\pi}{2}\xi\right)\, A(\bar{x}) \tag{34}$$

In this case it is found that

$$A(\bar{x}) = B_2 e^{-\delta_2 \bar{x}} \ ,$$

where

$$\delta_2 = \frac{\pi^2 Z k h U_*}{4L^2 U_0(Z)} \quad .$$

Then,

$$-\frac{U'}{U_0(Z)} e^{\delta_2 \bar{x}} = Q_2 B_2 \cos\left(\frac{\pi}{2}\xi\right) \quad . \tag{35}$$

and since presumably $U' = U_s$ when $\xi = 0$, $Q_2 B_2$ can be determined from a plot of the left-hand side of (35) against ξ.

Testing of Theory

Table 3 contains a listing of those data which were suitable for testing the theoretical development. Most of these data were measured when the instruments were 8 ft above the ground; however, on 6-6-76 the instruments were 15 ft above ground during runs 2 and 9, 30 ft above ground during runs 3 and 10, and 60 ft above ground during runs 4 and 11.

The third and fourth columns of Table 3 give the velocity components relative to a cartesian coordinate system in which x is in the direction of the reference wind (U_0) and passes through the center of the building; x = 0 was taken to be at the building wall on the downwind side. Columns 5 and 6 give the location of the observation point in this coordinate system. In this coordinate system observations at points outside of $y = \pm L$ do not have a defined x position. Therefore, some data appearing in Tables 1 and 2 do not appear in Table 3.

Experimental variability precluded a very good match of the observations with any of the theoretical relationships given previously. However, the most acceptable results were obtained using (35).

Table 3. - Wake Data

Date and Run	Tower	Relative Components U(m/sec)	V(m/sec)	Position x (ft)	y (ft)
	1	U_0 =	3.0	---	---
4-17-74	2	2.4	-0.2	131	-42.5
Run 8	3	2.2	0.2	123	- 3
	4	2.1	-0.7	122	36
	1	U_0 =	2.5	---	---
4-23-74	2	1.7	-0.5	190	-52
Run 1	3	1.0	0.7	92	1
	4	1.0	0.3	92	36
	5	1.5	-0.8	92	70.5
4-24-74	1	U_0 =	2.0		
Run 1	5	1.4	-0.5	140	-13
10-16-75	1	U_0 =	6.8	---	---
Run 1	4	-2.0	-2.5	45	-45.4
10-16-75	1	U_0 =	5.1	---	---
Run 2	2	0.0	-1.3	87	-54.7
	4	0.8	-2.7	87	-17.8
10-16-75	1	U_0 =	3.6	---	---
Run 3	2	3.0	-1.1	146	20.1
	4	4.1	-0.6	258	58.5
10-17-75	1	U_0 =	3.4	---	---
Run 1	4	-0.5	-1.0	45	-42.9
	5	-0.8	-2.7	45	- 6.6
10-17-75	1	U_0 =	5.2	---	---
Run 2	2	1.7	-1.4	88	10.6
	4	3.8	0.2	167	46.7
10-17-75	1	U_0 =	5.4	---	---
Run 3	2	1.1	-1.9	163	-63.6
	4	4.4	-1.8	163	-34.2

Table 3. - Continued

Date and Run	Tower	Relative Components U(m/sec)	V(m/sec)	Position x (ft)	y (ft)
10-17-75	1	U_0 = 6.0		---	---
Run 5	4	4.0	-2.2	202	-49.1
10-17-75	1	U_0 = 5.3		---	---
Run 6	2	0.2	-2.2	77	-45.3
	4	3.4	-2.3	155	-57.1
6-6-76	1	U_0 = 2.9		---	---
Run 1	2	2.8	0.2	239	47.8
6-6-76	1	U_0 = 3.5		---	---
Run 8	2	2.7	-0.4	194	-37.1
6-6-76	1	U_0 = 3.2		---	---
Run 2	2	2.6	-0.4	247	58
6-6-76	1	U_0 = 3.7		---	---
Run 3	2	4.0	-1.0	278	79
6-6-76	1	U_0 = 3.2		---	---
Run 4	2	3.5	-0.7	251	42
6-6-76	1	U_0 = 3.6		---	---
Run 9	2	2.6	0	179	13
6-6-76	1	U_0 = 3.2		---	---
Run 10	2	3.0	0.2	208	-52
6-6-76	1	U_0 = 3.8		---	---
Run 11	2	3.9	-0.1	195	-25

Figure 5 shows a plot of $- U'e^{\delta\bar{x}}/U_0(Z)$ vs. ξ, where

$$\delta = \frac{k^2 h \pi^2 Z}{4L^2 \ln Z/z_0} \quad ,$$

and z_0 was estimated to be 0.1 ft. The points shown as solid dots in Figure 5 are the only ones which are considered valid for purposes of testing the theory. These are the only points that satisfy the assumption of the theory that U' should be small compared to U_0. The curve $\xi = 0.4 \cos(\pi\xi/2)$ has been drawn as a suggested fit to these points - it has not been verified by the least-squares procedure.

The reason the other points have been ignored also can be illustrated by reference to Figure 6 which shows wind vectors, normalized by division of the magnitude by U_0, at the various observation points in the x-y coordinate system. This figure is only roughly representative of the flow that might be expected with simultaneous observations at many points. Obviously it does not account for variations in the shape of the cavity and the structure of the wake flow with variations in the orientation of U_0 relative to the building, as shown by Evans (op. cit.). However, certain features in Figure 6 are indicative. For example, the points shown by crosses must represent observations within or very close to the cavity. The theory on the other hand was developed for the region downwind from the cavity. The observations with solid dots in Figure 6 correspond to those shown by solid dots in Figure 5, which indeed are downwind of the cavity region.

The points shown by open squares in the two figures are observations which seem to be in a transition region between the cavity

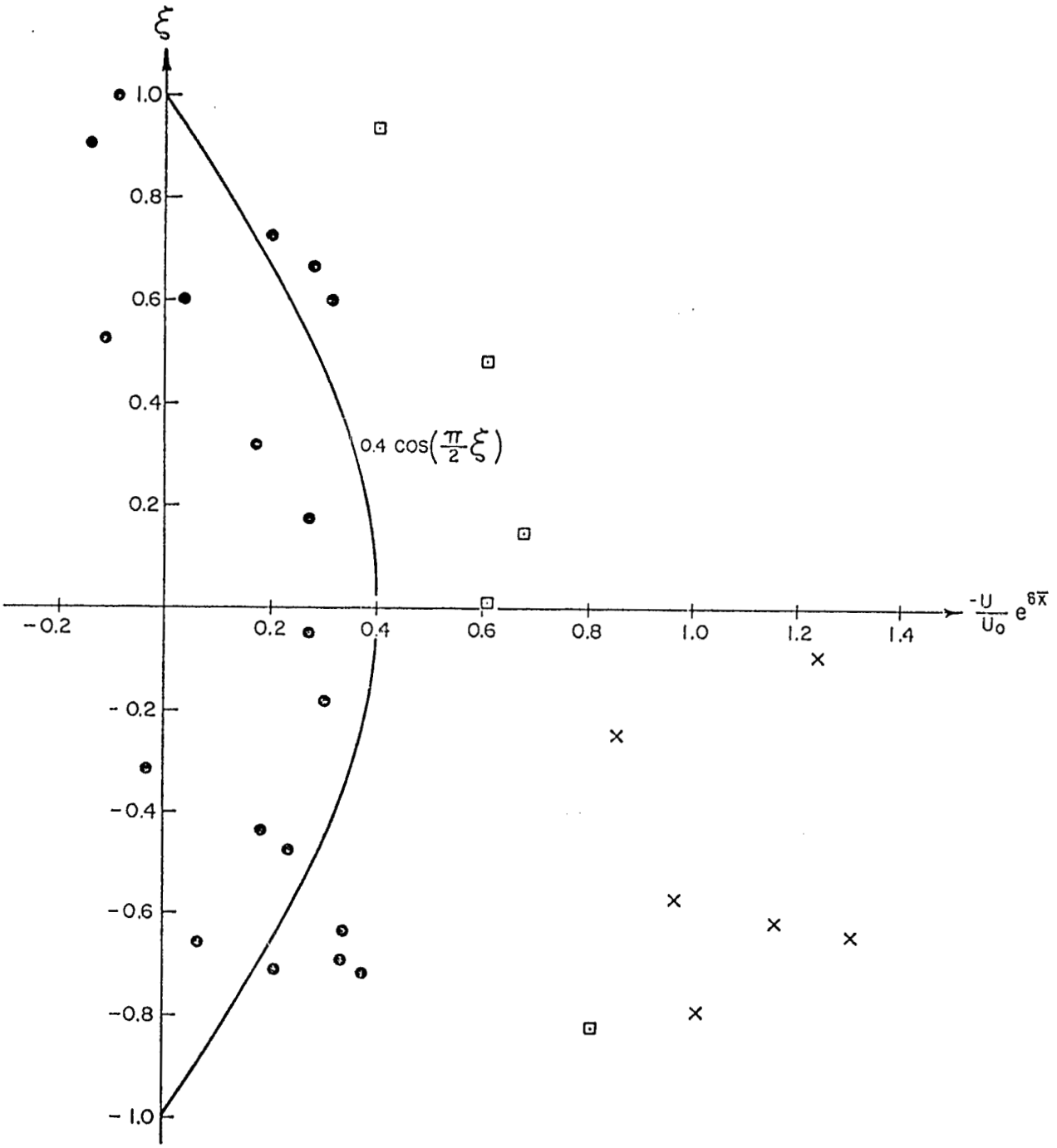

Figure 5. - A plot of ξ vs. $-\frac{U'}{U_0(Z)} e^{\delta \bar{x}}$ using the data in Table 3;

$$\delta = \frac{\pi^2 k^2 h Z}{4L^2 \ln(Z/z_0)}$$

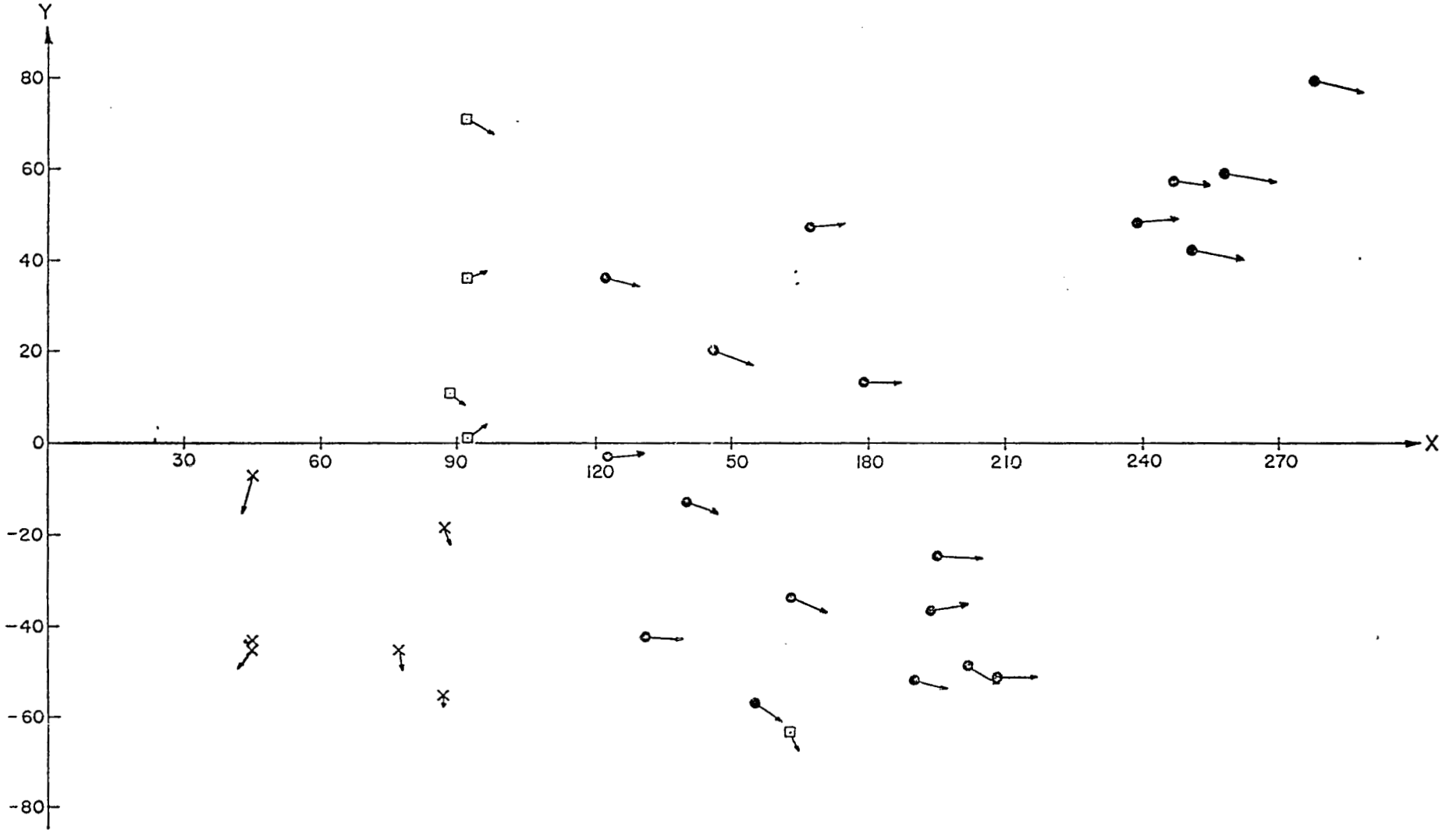

Figure 6. - Normalized wind vectors in the x-y plane, disregarding the orientation of the reference wind relative to the structure.

and the remainder of the wake flow. These observations also fail to meet the criterion that U' be small compared to U_0. The theory appears to become valid for values of x greater than 100 to 120 ft. This corresponds in the present case to values of $\overline{x}$ of 2.5 to 3.

It should be pointed out that we were unsuccessful in obtaining usable observations at distances greater than seven building heights. This was because when working at these distances and moving the instruments about, the natural variability of the wind makes it difficult to guess where the boundaries of the wake will be in the mean.

CONCLUSIONS

Based upon scaling and dimensional analysis, the statement

$$-U' = U_0 \, \beta \cos(\pi\xi/2) \, e^{-\delta\overline{x}} \quad ,$$

was derived for the flow in the wake of a building at points downstream of the cavity. In this statement, β is a constant with a value of about 0.4 and δ depends upon the orientation of the undisturbed mean flow relative to the building. The vertical dimension of the structure is accounted for in $\overline{x}$ and the lateral dimension is approximated in ξ.

The foregoing relationship appears to be a reasonable fit to the observations; however, there is a large degree of experimental variability and additional observations, especially at distances greater than seven building heights, are needed to provide complete verification.

The results indicate that an aircraft passing through the wake during take-off or landing would experience not only a change in turbulence level, but a change in mean wind speed of a magnitude roughly equivalent to that of the eddy components.

An interesting difference between the results of wind tunnel studies and those obtained here is with regard to the bubble or cavity. Depending upon the author, reattachment has been found in model studies to occur seven or more obstacle heights downstream. Evans' (op. cit.) results are the exception. For a building of the size and shape of the hangar involved in this study, his results indicate that reattachment should have occurred about two and a half building heights downstream. Our results are in good agreement with this.

ACKNOWLEDGMENTS

The author gratefully acknowledges the help freely given him during the course of this study by the following individuals:

Dr. V. Thomas Rhyne, Associate Professor of Electrical Engineering, and his students for providing the computer program, equipment, and help to do the conversion of the data from analog to digital form.

Mr. Joe Janac, electronics technician, for his help in installing and trouble-shooting the recording equipment.

David Dar-Way Chu, graduate student, who was supported by the project for a short time as a research assistant, but who gave many hours without pay in the observation program and doing the data reduction.

Mrs. Janie Leighman for typing this manuscript.

The Texas Transportation Institute and the Texas State Highway Department for the use of the 60-ft towers used in the study.

REFERENCES

Calder, K. L., 1967: Concerning similarity analysis based on the use of governing equations and boundary conditions and Long's method of generalized dimensional analysis. J. Atmos. Sci., 24, 616-626.

Colmer, M. J., 1971: Some full-scale measurements of the flow in the wake of a hangar, Aeronaut Res. Council C. P. No. 1166, Her Majesty's Stationery Office, 28 pp.

Counihan, J., J. C. R. Hunt, and P. S. Jackson, 1974: Wakes behind two-dimensional surface obstacles in turbulent boundary layers. J. Fluid Mech. 64, 529-563.

Evans, B. H., 1957: Natural air flow around buildings. Res. Rept. No. 59, Texas Eng. Exp. Station, A&M College of Texas, 13 pp.

Frost, Walter, 1973: Review of data and prediction techniques for wind profiles around manmade surface obstacles, Project Report for NASA Marshall Space Flight Center, CRNA8-27387, 18 pp.

Frost, Walter, J. R. Maus, and W. R. Simpson, 1973: A boundary layer approach to the analysis of atmospheric motion over a surface obstruction, NASA Project Rept., CR-2182, 141 pp.

Halitsky, James, 1968: Gas diffusion near buildings, Meteorology and Atomic Energy, David H. Slade, Editor.

Hirt, C. W., and J. L. Cook, 1972: Calculating three dimensional flows around structures and over rough terrain, J. Comp. Phys., 10,324-340.

Hotchkiss, R. S., 1971: The numerical calculation of three-dimensional flow of air and particulates about structures, Proc. Symp. on Air Pollution, Turble and Diff., Las Cruces, N. M., 35-42.

Hunt, J. C. R., 1972: Some theories for the mean and turbulent velocity distributions in flows around bluff bodies. Symposium on External Flow, University of Bristol, 10 pp.

Jones, J. G., 1969: The speed response of an aircraft constrained to fly along a straight path in the presence of turbulence at low altitude, Aeronaut. Res. Council R. & M. No. 3563, Her Majesty's Stationery Office, 27 pp.

Kaynes, I. W., 1971: Aircraft center of gravity response to two-dimensional spectra of turbulence, Aeronaut. Res. Council R. & M. No. 3667, Her Majesty's Stationery Office, 35 pp.

Long, R. R., 1963: The use of the governing equations in dimensional analysis. J. Atmos. Sci., 20, 209-212.

Plate, E. J., 1971: Aerodynamic Characteristics of Atmospheric Layers. USAEC Division of Technical Information Extension, Oak Ridge, Tennessee, 190 pp.

Sexton, D. E., 1971: Discussion of effects due to groups of guildings, Phil. Trans. Roy. Soc. Lond. A., 269, 483-484.

Tennekes, H., and J. L. Lumley, 1972: A First Course in Turbulence, the MIT Press, Cambridge, Massachusetts, 300 pp.

Thomas, J. C., 1971: On air flow in the vicinity of tall buildings in downtown Houston, Texas. Ph.D. Dissertation, Texas A&M University, 105 pp.